Modeling of a prestressed concrete bridge with 3D finite elements for structural health monitoring using model updating techniques

S. Schommer[1], T. Kebig[1], V.-H. Nguyen[1], A. Zürbes[2], S. Maas[1]
[1] University of Luxembourg, Faculty of Science, Technology and Communication
6, rue Richard Coudenhove-Kalergi, L-1359, Luxembourg, Luxembourg
[2] Bingen University of Applied Sciences, Department 2
Berlinstraße 109, D-55411, Bingen am Rhein, Germany
e-mail: **tanja.kebig@uni.lu**

Abstract
This paper presents a linear finite element model for a prestressed concrete beam, which was part of a real bridge. Static and dynamic tests were carried out and compared to the numerical simulation responses. A solid finite element model was created including the prestressed concrete beam, permanent dead load, two additional live loads and a shaker. A well planned finite element model is very important for later detection and localization of damage. Therefore, a mapped mesh was used to define so-called 'slices', which enables describing stiffness changes, e.g. damage. The model validation was performed by comparing simulated results to measured responses in the healthy state of the beam. After validation of the reference model, it is possible to modify the bending stiffness along the longitudinal axis of the beam by modifying Young's moduli of different slices to adapt for the effect of damage.

1 Introduction

Model updating is often used for damage detection in civil engineering structures. Prerequisite is a parameterized model using finite element method to validate at first the healthy reference state. For a successful damage assessment, the reference model has to present the real structure as accurately as possible. The model updating includes a complex procedure, containing also model errors resulting from idealizations and assumptions. On the other hand, measurements of physical properties are never absolutely accurate due to measurement uncertainty. An elaborated review on numerical and application aspects for model updating was reported in [1]. It described the choice of updating parameters and the definition of residuals, which may be used to compare the physical measurements and analytical results. The difference between measured and simulated physical quantities may be reflected by a weighted sum of the residual vector which is the core of an objective function. An optimal model parameter set can be found to minimize this function.

The number of parameters to be updated is often an important issue as it largely influences the computational cost or the convergence. The definition of 'damage function', proposed by Abdel Wahab et al. [2], allows reducing efficiently the number of parameters. The technique was further developed by Teughels et. al. [3] by combining element groups and using dimensionless parameters. As revealed clearly in its name, damage function can describe mathematically a damage for example by modeling stiffness reduction. In [3, 4], damage localizations were carried out with beam models and a number of damage functions summing up Legendre polynomials.

The present study examines a part of a real prestressed concrete bridge in Luxembourg that artificial damage was provoked with increasing severity. Static and dynamic responses were measured in each damage scenario. Further than the simple beam models in [3, 4], the damage localization is here performed with a more detailed solid model including prestressed tendons. Moreover, only one damage function was used,

based on a Gaussian Bell curve, which enables a fast model updating procedure. Differences between model responses and measurements are assessed and summed-up in an objective function, which depends of course on chosen parameters. At a second stage, a set of measurements is considered and the model is updated by varying parameters in order to minimize the objective function. It is recommended to keep the number of parameters low to reduce computational effort and to achieve convergence. But the focus of the present paper is the generation of the solid model and its important features for its later use in model updating with damage functions.

2 Test set-up

The tests were carried out on a part of a real prestressed concrete bridge. The original bridge crossed the river Mosel between Grevenmacher (Luxembourg) and Wellen (Germany). Built from 1953 to 1955, the bridge was demolished in 2013 for safety reasons. It was a 5-span bridge and each field composed of 5 adjoining concrete T-section beams. These beams were prestressed by internal steel tendons in longitudinal direction.

For the test set-up, two of these beams with a length of 46 m and a mass of approximately 120 t each, were transported to the port of Mertert (Luxembourg). One of them with 19 tendons was used as the test beam and was supported at the two ends by a sliding and a fixed bearing. For the fixed bearing, the beam was molded with concrete and the sliding bearing was realized by two steel plates. Grease was spread between the two steel plates to reduce the friction. Before the demolition of the original bridge, the asphalt layer had been removed. However, a purpose of the test was to reproduce the condition during the lifetime of the bridge as far as possible. A part of the second beam with a length of 12 m and a weight of about 30 t was used to simulate an additional dead load due to the removed asphalt layer. Live load due to traffic was represented by two additional loads of about $2 \cdot 13$ t = 26 t put on top of the test beam. During the static tests with the live loads, the additional dead load stayed on top of the beam. For vibrational testing, an electromagnetic shaker was positioned between the additional dead load and the live loads. The whole test set-up is shown in Figure 1.

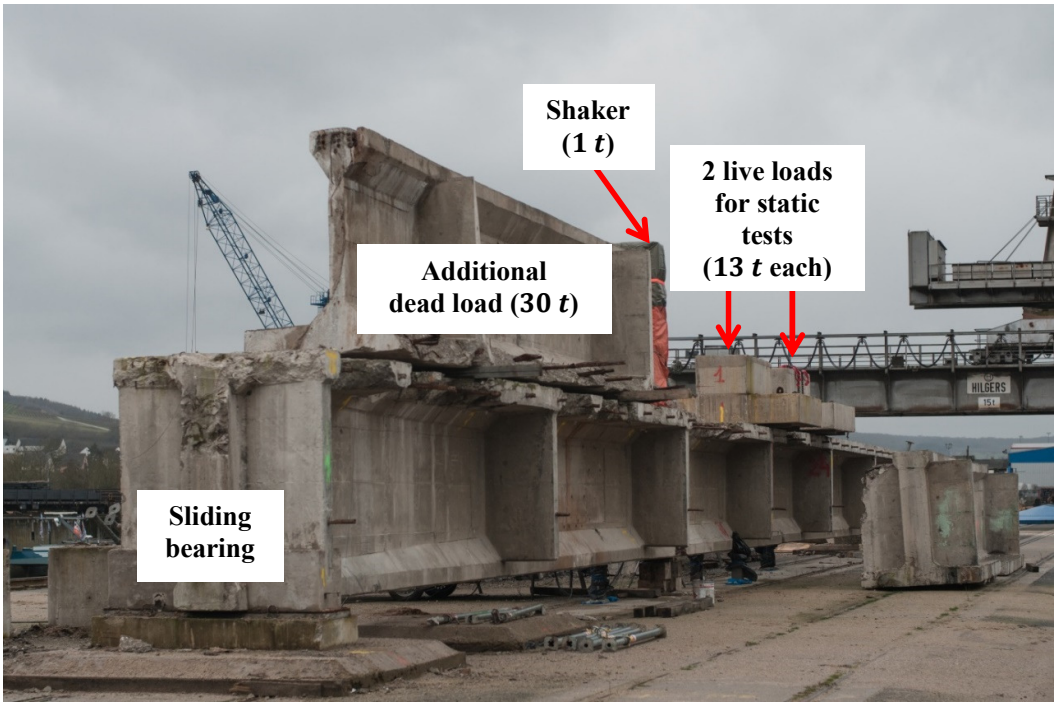

Figure 1: Test set-up at the port of Mertert

The beam was equipped with 8 displacement transducers, 8 temperature sensors and 26 accelerometers for the vibrational testing. The location of the sensors is presented in Figure 2. During the whole test period of about 1 month, the vertical deflection versus ground was recorded by 7 transducers (SV1-SV6, SV8) at the bottom of the beam. Another sensor (SH7) was attached to register horizontal displacement of the sliding bearing. In addition, the concrete temperature (T1-T7) and the ambient air temperature (T_{amb}) were measured.

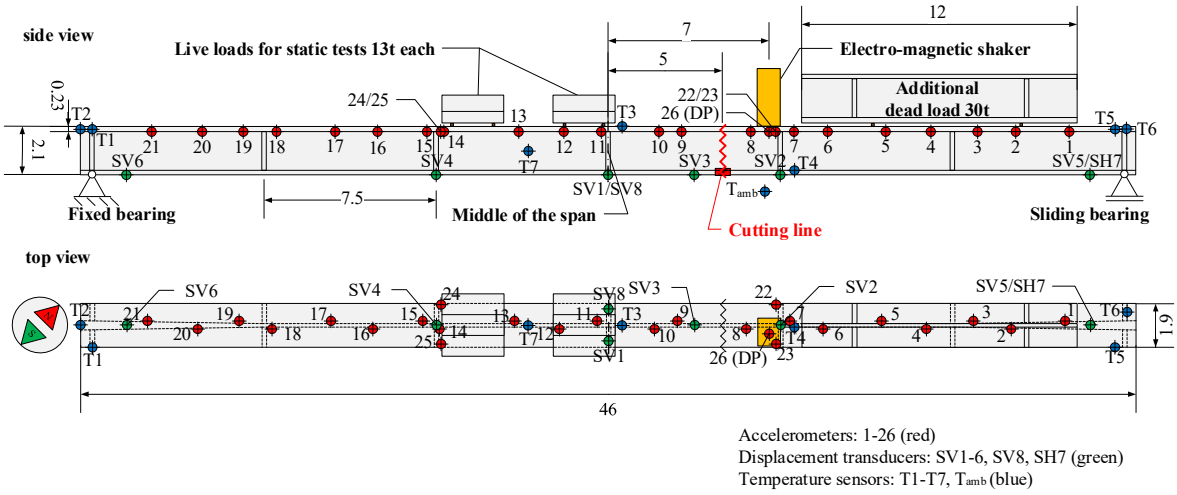

Figure 2: Side and top view of test set-up with sensors

Artificial damage was applied in 4 steps by cutting tendons at a distance of 5 m off the middle of the beam, as shown by the cutting line in Figure 2. Hence, totally 5 pre-defined damage scenarios (DS) were studied. The first DS#0 represents the undamaged reference state and DS#4 the most severe damaged state of the beam. DS#1 to DS#4 correspond to the cutting of 2, 4, 6 and finally 9 tendons. The damage was always introduced symmetrically on both sides of the beam. Figure 3 demonstrates the lower part of the cross-section at the damage location with the position of the 19 tendons. In the last scenario DS#4, 6 tendons were only partly cut, when clearly visible cracking was observed. Fully cut cables are marked by a cross, while a partially cut is marked by a half-filled circle.

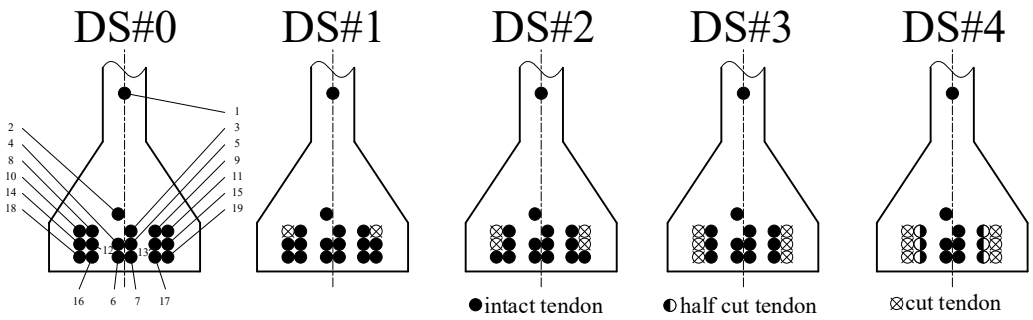

Figure 3: Damage scenarios

3 Finite Element (FE) Model

The measurements were analyzed and used for a model updating procedure based on a parameterized FE-model in order to identify local stiffness reduction. Hence, the chosen parameters should be able to represent stiffness reductions in the model. Damage may be evaluated by tracking the selected parameters starting from the initial model in the healthy state. The main characteristics of the T-shaped cross-section of the beam are shown in Figure 4.

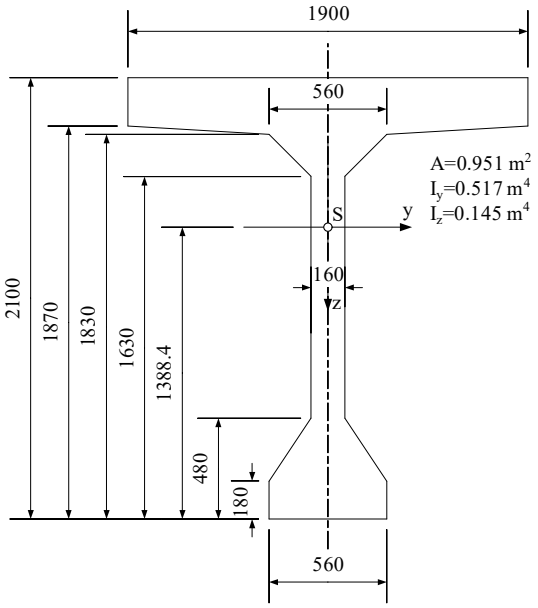

Figure 4: Cross section of the beam in the middle of the span (dimensions in [mm])

A finite element model was prepared with ANSYS Classic 17.0. The Ansys Parametric Design Language (APDL) was used to create the parametric model and to implement batch processing allowing large numbers of automatic simulations that optimization often requires. Therefore, a linear model was chosen. In addition to linear elastic material models, the contact conditions were defined in a way so that no nonlinearities (e.g. contact) occurred in the model. A volume model of the test set-up was created with mainly solid elements. Table 1 shows the most important elements used in the model.

Type	Description	Node number	Usage	Important options
SOLID186	Structural Solid	20	Hexahedral elements for mapped meshing	Sometimes used as tetrahedral- or as pyramid-shaped elements
BEAM188	Beam	2	Beam elements for the tendons, Dummy-Beams to connect the tendons to the concrete	Timoshenko beam theory
MPC184-Revolute	Multipoint Constraint Element, Revolute Joint	2	To model a revolute joint at the sliding bearing	
MPC184-Planar	Multipoint Constraint Element, Planar Joint	2	To model a planar joint without friction at the sliding bearing	

Table 1: Element types

A local stiffness loss due to cracking or reduction of stiffness along the beam's length can be simulated by reducing YOUNG'S modulus. The idea was to split the beam into narrow "slices", whose stiffness can be reduced as a whole to limit the number of free parameters. This was implemented by a mapped mesh. "SOLID186" – a hexahedral element with 20 nodes and with "brick" shape was used allowing an easy definition of slices. Each slice can be defined and assigned with its own material. At the beginning, the material properties were uniform and Young's moduli can be modified during the model updating. The mapped mesh does not only reduce the number of elements compared to a free mesh but also avoids distorted elements and thus increases the mesh quality.

Figure 5 illustrates the mapped meshing with solid elements, e.g. around the sliding bearing side. Different colors present different materials and material properties can be varied individually. In the present model, the beam was divided into 227 individual "slices" of 20 cm thickness. The YOUNG's modulus of the concrete was initially set to 30.000 MPa and for the steel tendons to 200.000 MPa.

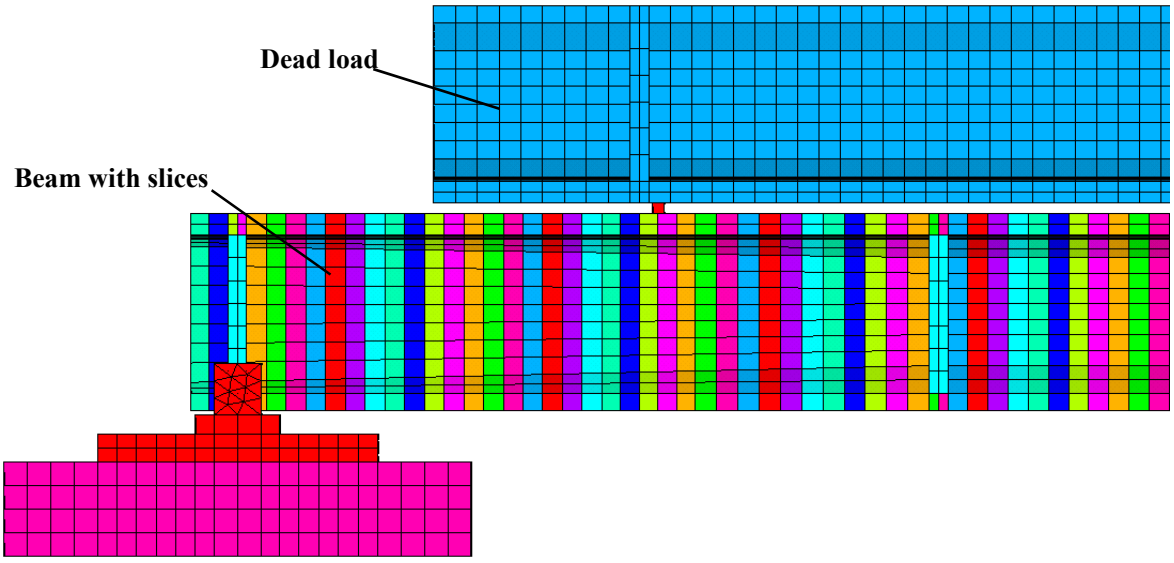

Figure 5: FE-model of the test set-up with mapped mesh; diverse colors show different materials

The tendons in longitudinal direction were also simulated and meshed with the concrete beam. In reality, each tendon consists of 12 individual round bars with a diameter of 7 mm. They were arranged in a thin jacket pipe and held in position by a spiral spring. After a pre-tensioning the tendons were grouted as illustrated in Figure 6. In this model, a tendon is represented by a pipe with area and moment of inertia equivalent to the ensemble of 12 round bars. It was assumed here that the round bars did not move relatively to each other due to the grouting. Thus, the tendons were simulated by pipe with an inner diameter di = 21.4 mm and an outer diameter da = 32.4 mm.

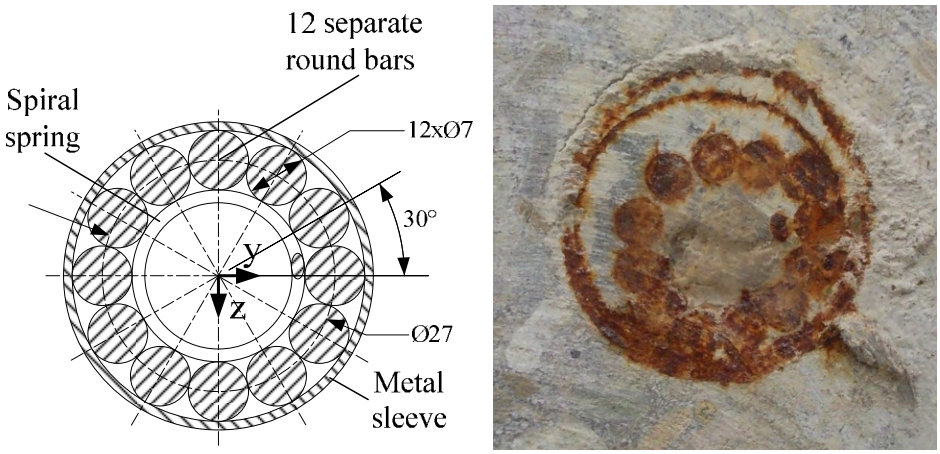

a) drawing with dimensions

b) photo of a real tendon of a cut beam, filled with mortar

Figure 6: Cross section of the tendons

Then in order to connect the tendons to the surrounding concrete elements, node-to-node connections were created by additional dummy (beam) elements as detailed in Figure 7. Those dummy elements had material properties like the tendons, but zero density, and hence they added no mass to the system. As a beam element has 6 Degrees of Freedom (DOFs) per node and a solid element has only 3 translational DOFs, the 3 rotational DOFs of a beam element remain free in such a connection. To solve this problem, each node of the tendons was in addition connected to 3 nearest neighboring nodes of concrete (solid) elements. These multiple connections allow transmitting moments between the connected elements. An overview of the prestressed-tendons is shown in Figure 8.

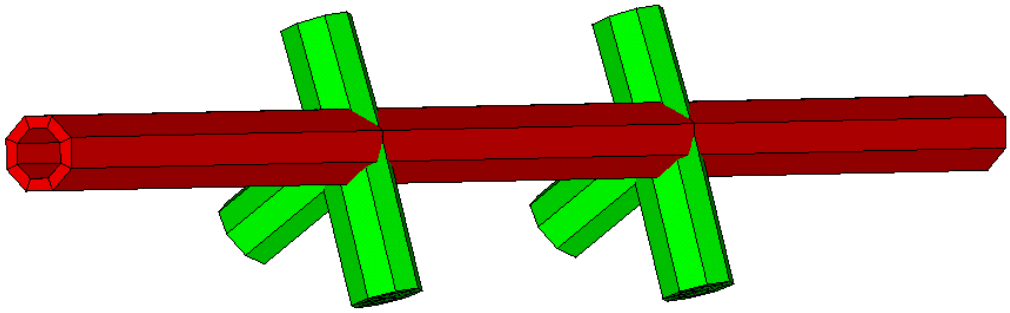

Figure 7: Part of a tendon (red) with additional dummy beam elements (green) connecting it in the model to the concrete

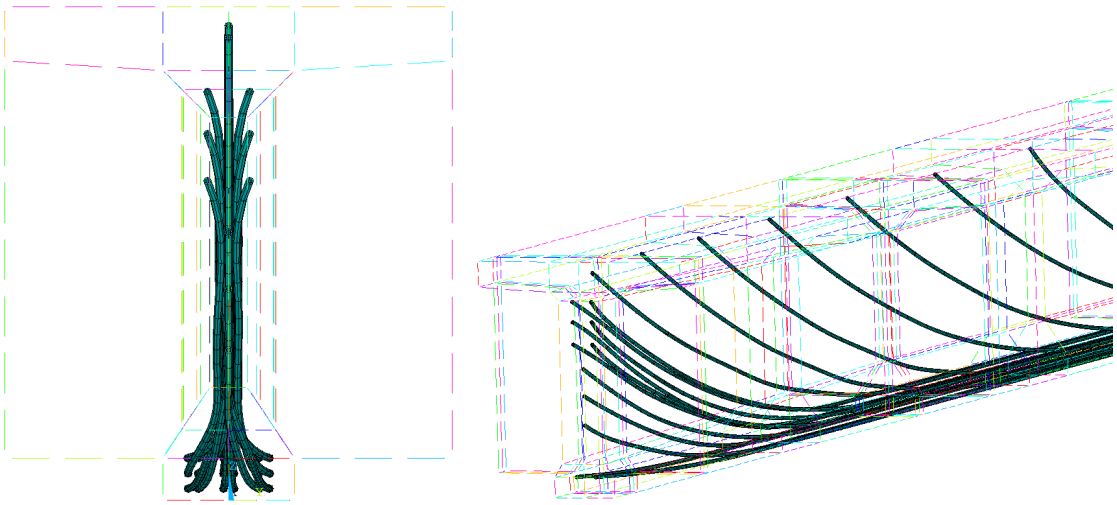

Figure 8: Internal tendons inside the test beam

Then the permanent additional dead load of 30 t was also modeled by elements without intermediate nodes (SOLID185). The last step concerns the modeling of the bearings. The bridge part was set up as a simply supported beam but in reality, the fixed bearing and especially the sliding bearing did not show behavior of ideal bearings. On the fixed bearing, the beam was surrounded by concrete for a length of about a half meter. So it was not only supported at one point, but in a certain area. The concrete of the bearings was quite young and hence not completely rigid. Therefore, a rotation around the transverse axis was possible but not completely free. The sliding bearing was realized by two steel plates with grease between. The cast concrete including the foundation and a part of the soil were also modeled as volume elements. In addition to the contact between these volume bodies, the contact between the bearings and the beam had to be defined. Therefore, surface contact elements with the "always bonded" option were used for both bearings, which hence merged the two FE-meshes. Furthermore for the sliding bearing, additional movement possibilities had still to be modeled. Therefore two joints were simulated by using elements of type MPC184-revolute and -planar joint. Nonlinearity can be avoid by switching off the alteration of underlying constraint equations in case of large deformations for the MPC184-elements. The soil under a bearing was modeled by a cube as shown in Figure 9. To fix the soil, the movements of 3 surfaces of this cube were blocked in the direction perpendicular to the surfaces. As the sliding bearing was not perfect, its horizontal displacement was blocked for the dynamic test due to friction, while the friction was zero for the static loading. For this phase, elements of type MPC184-planar was changed by MPC184-rigid.

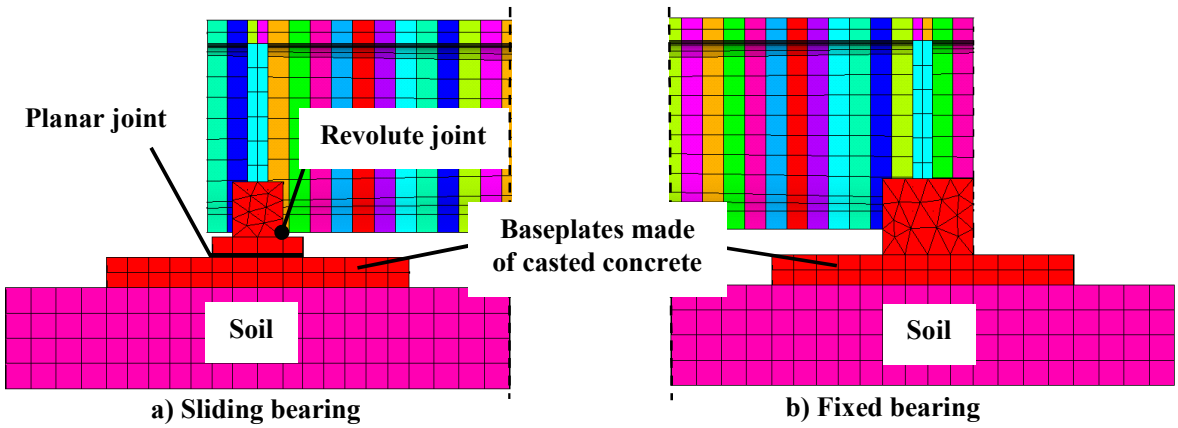

Figure 9: FE-models of the bearings

The shaker used for vibration tests was represented by a lumped mass. Furthermore, 'live loads' including two 13 t weights put on the beam only for static loading tests were also considered. Their weight was represented by pressure load on the contact area between two supporting wooden beams and the tested concrete bridge. The present paper does not describe the model updating procedure and its criteria in detail, which will be done in another paper. The focus is here the modeling itself: solids clustered in slices with a mapped mesh and beams for the tendons.

4 Model Validation

The validation of the model is performed by comparing simulated results to the measurements in the healthy state (DS#0). Figures 10-15 present the simulation in comparison to the measurements. The first result shows the deflection in a loaded state. Figure 10 reveals that the measured and the simulated results match well. The measured displacements had been compensated for temperature effects, which is detailed in a former paper [5].

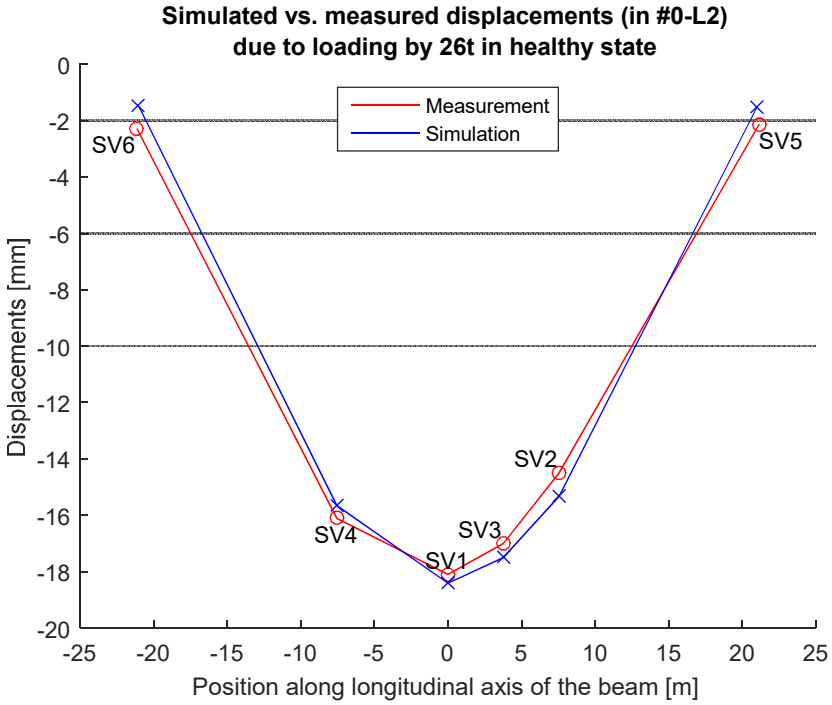

Figure 10: Comparison of the measured deflection in a loading - healthy state due to test weights and simulated vertical displacements

Results of the modal analysis are displayed in the following. The first simulated mode is bending in the horizontal plane, i.e. x-y plane in Figure 11, however this mode was not identified by the Experimental Modal Analysis (EMA), as only vertical DOFs were measured. The second simulated mode at 3.00 Hz shown in Figure 12 is a vertical bending mode, which could be correlated to the measured mode named B1, identified at 2.88 Hz. The correlation based on Modal Assurance Criterion (MAC) between these two mode shapes led to a good value with MAC = 0.982.

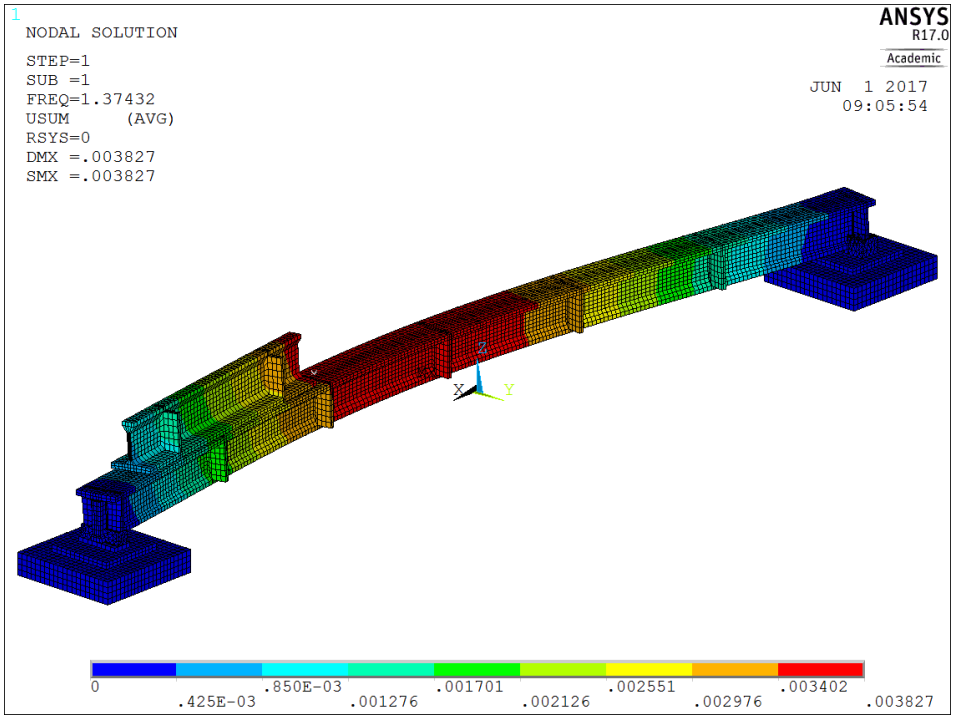

Figure 11: Bending mode in y direction at 1.37 Hz

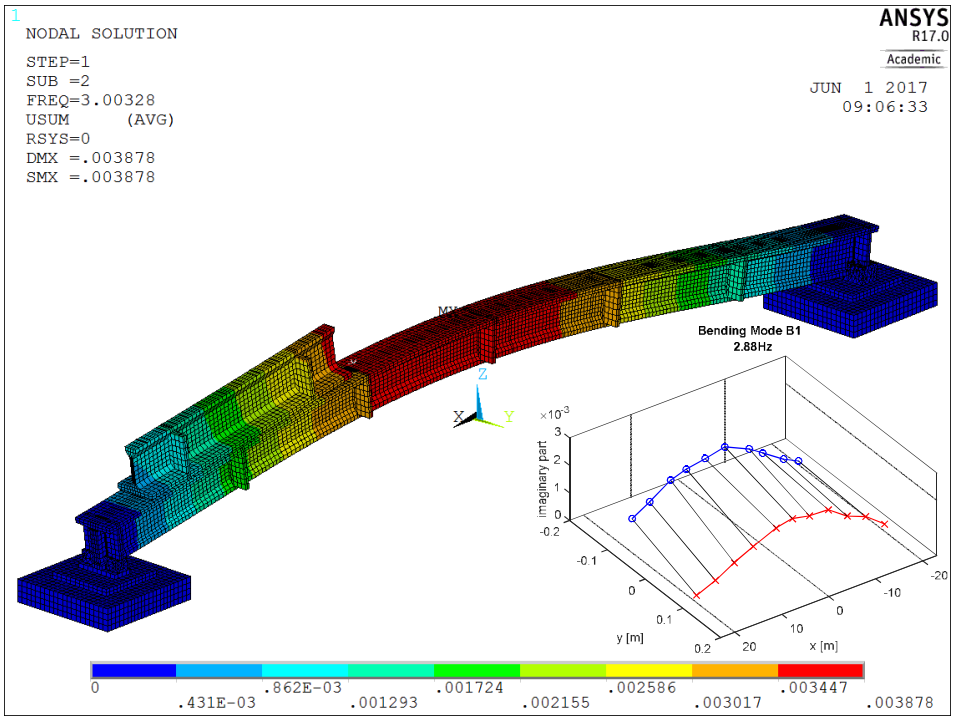

Figure 12: Simulated bending mode at 3.00 Hz juxtaposed with measured mode B1 at 2.88 Hz (MAC = 0.982)

The next two simulated modes are torsional; mode at 5.21 Hz correlated with mode T1 measured at 4.48 Hz. Torsional modes were not well identified in the EMA, because the sensors were positioned too close to the middle of the web of the beam, resulting in inadequate MAC values.

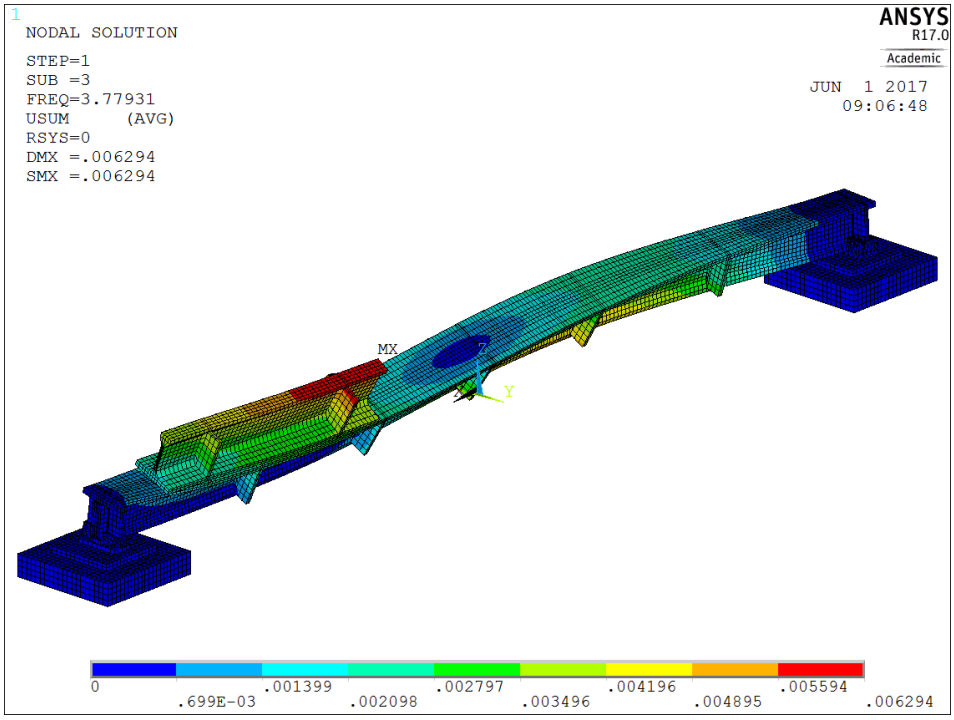

Figure 13: Torsional mode at 3.78 Hz

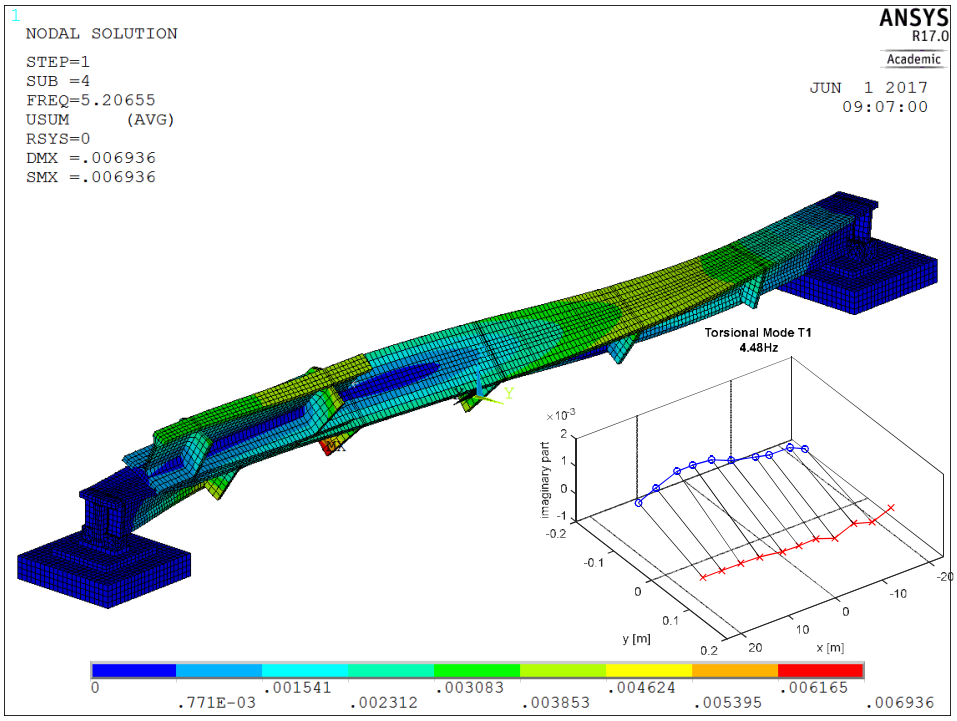

Figure 14: Simulated torsional mode at 5.21 Hz compared with mode T1 measured at 4.48 Hz (MAC = 0.632)

The correlation between simulated and experimental modes scores better with the next bending mode as shown in Figure 15. In the next step of model updating, 3 modes B1, T1 and B2 shown in Figure 12, 14 and 15 are used with their corresponding MAC values and eigenfrequencies.

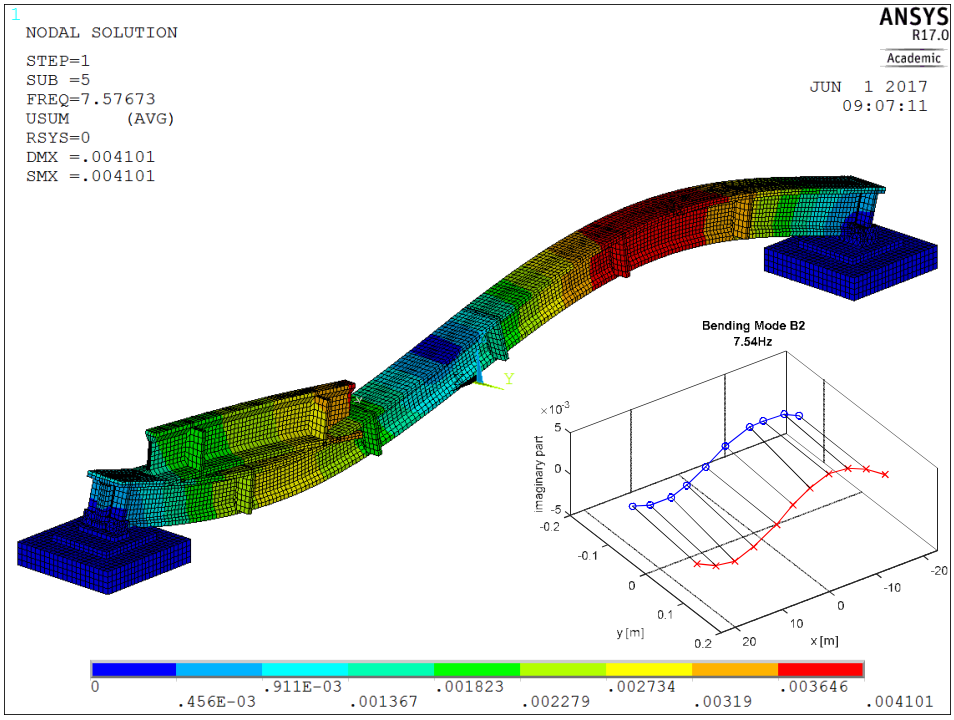

Figure 15: Simulated bending mode at 7.58 Hz correlated with mode B2 measured at 7.54 Hz (MAC = 0.970)

After the validation of the initial reference model, the effect of damage can be simulated by modifying the bending stiffness along the longitudinal axis of the beam. This is done by changing Young's moduli of the predefined slices. Totally 227 slices in the model lead to 227 parameters that describe the bending stiffness. This number of free parameters is too large for updating and hence has to be reduced. An interesting approach is 'damage function', introduced by Abdel Wahab et al. [2], Teughels et. al. [3]. It consists in using dimensionless parameters and in combining element groups and so that only some parameters of these groups are used for the updating. The damage function uses a predefined pattern reflecting the influence of damage on stiffness. It thus enables a physically reasonable optimization with reduced number of variables. Those damage functions are described and discussed in our former works [6, 7] and are not presented in detail in this paper.

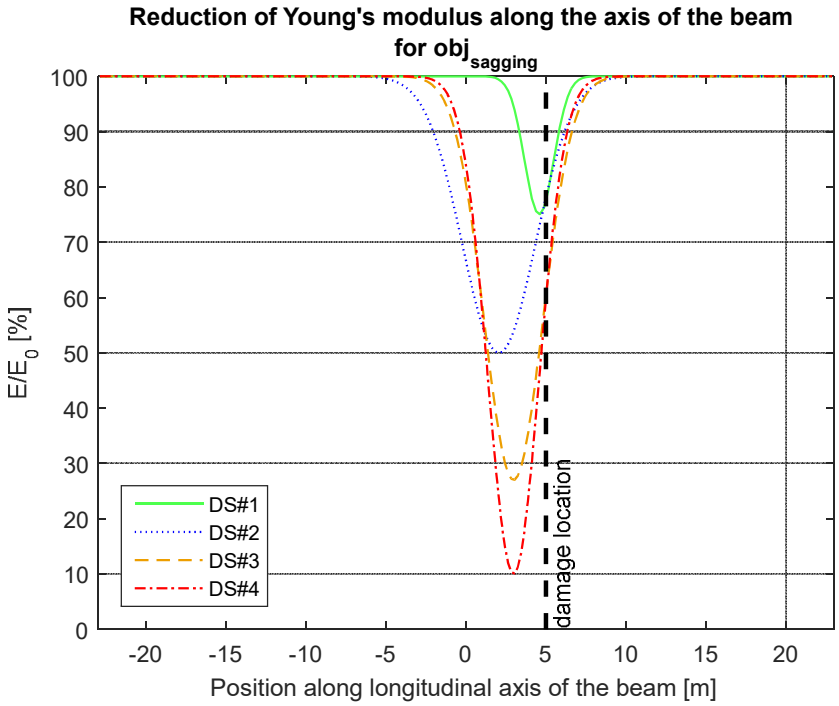

Figure 16: Reduction of Young's modulus along the longitudinal axis by the optimal parameter sets

In our current model, the slices have an axial length of about 20 cm and so lead to a quite coarse localization of damage. The results given in Figure 16 and distinguish well the level of stiffness reduction and show the damage locus near the cutting line. The abscissa presents the length of the beam that the origin is defined in the middle and the cutting line is 5 m off the origin.

In order to improve the accuracy of the localization, the axial widths of the slices need to be reduced. As the width of a crack is only in the order of magnitude of millimeters, the mesh has to permit very local stiffness reduction. On the other hand, a large stiffness reduction occurs directly at the location of a crack due to the diminution of the cross-section. But at only small distance from the crack, the cross-section is intact again. In the current work, a damage function with the shape of a Gaussian Bell curve was used, which is given by

$$p \cdot e^{-0.5\left(\frac{x-\mu}{\sigma}\right)^2} \tag{1}$$

Hence the 3 parameters describe damage provided the axial mesh is sufficiently fine: p for the maximal reduction, σ for the width of the curve and μ for localization. With a finer mesh, we can define a more narrow bell curve, that allows a more accurate localization of damage. Of course, any reduction of the element size evolves higher computing effort.

As the outputs from the coarse meshing provide us already a coarse localization of damage, the mesh at the identified location can be refined. The idea was carried out with a second model with refined mesh in a region of 1 m left and right of the cutting line. The axial width of slices was there reduced to 10 mm in the middle of this region as shown in Figure 17. To avoid skewed elements with large ratio of height to width, the element size in the vertical direction were also reduced. Simultaneously a transition needs to be created between the refined and the coarse mesh. For this purpose, a transitional mesh was generated with the same elements of SOLID186, however with tetrahedral or pyramidal shapes. The resulting mesh in the refined region is shown in Figure 17.

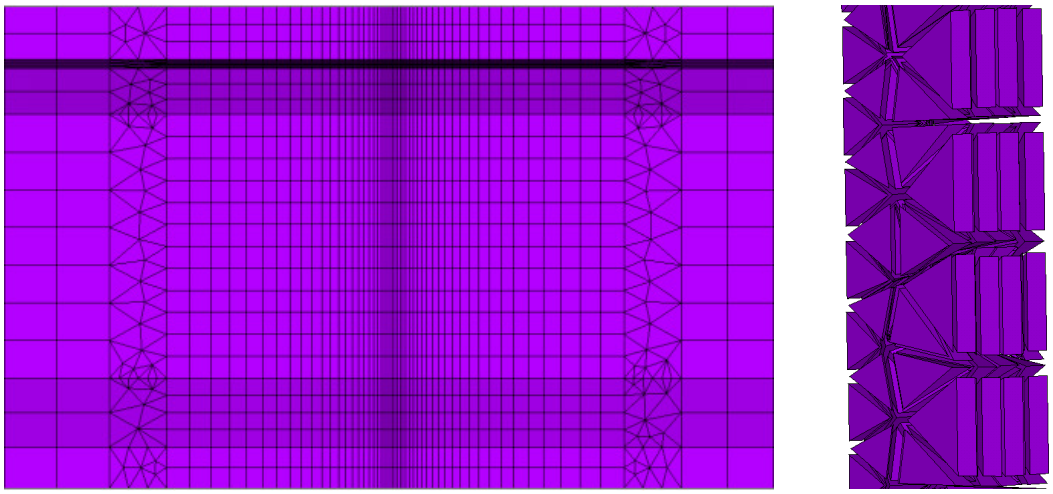

a) Refined mesh **b) Transition mesh shown with shrinked elements**

Figure 17: Mesh refinement in the refined region

This refined mesh leads to a more accurate damage localization, as shown in Figure 18. The damage was localized exactly at 5 m off the middle of the beam for state DS#1, DS#3 and DS#4; corresponding exactly to the cutting line. Only in DS#2, there is a little deviation of less than 20 cm due to convergence issue. However, by considering the whole length of the beam, the detection based on the refined mesh gives good results.

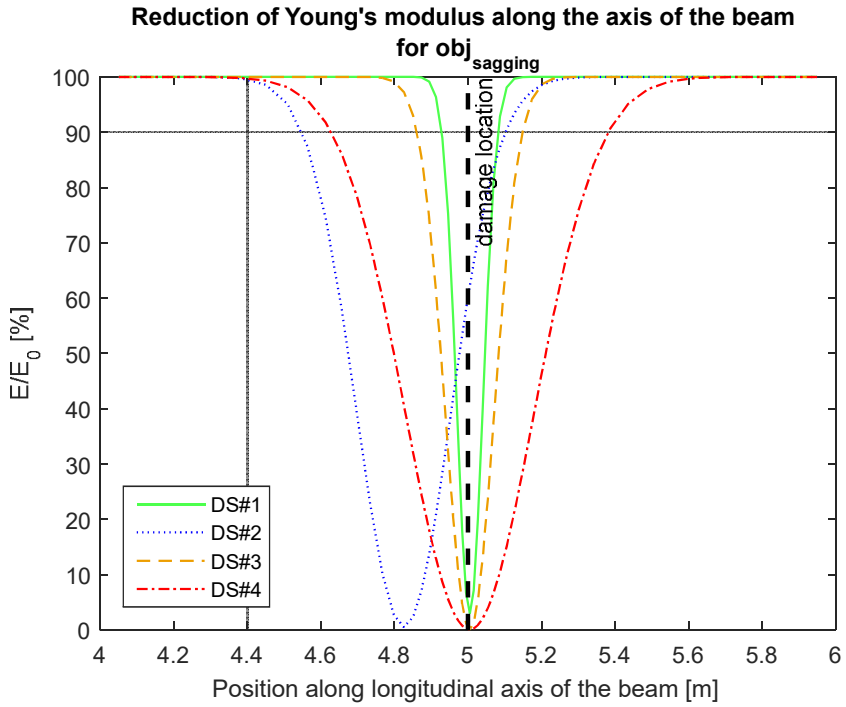

Figure 18: Reduction of Young's modulus along the beam in the refined FE-model

5 Conclusion

A part of a prestressed concrete bridge was tested in the presented work. The test-structure was exposed to real environmental conditions, such as temperature fluctuations and solar radiation, so the assessment was confronted with the same challenges as testing of a bridge still in operation. The FE-model consisting of solid elements allowing better accuracy than a classical simple beam analysis. An advantage is the mapped mesh allowing reduction effectively the computation cost and furthermore splitting the beam into controllable narrow slices. In this manner, it was possible to reduce the YOUNG's modulus of groups including adjacent elements to simulate the decrease of local stiffness due to cracks or reduction of the bending stiffness along the length of the beam.

Regardless of nonlinearities presented in bridges, the current work choose a linear FE-model for reasons of efficiency and practical application. Therefore, the model can be improved by considering nonlinearities, for instance on contact conditions. Another perspective relies to substructure-techniques that could reduce the computational effort.

References

[1] M. Link, *Updating of analytical models – review of numerical procedures and application aspects,* In: Proc., Structural Dynamics Forum SD2000, Research Studies Press, Baldock (1999), pp. 193-223.

[2] M.M. Abdel Wahab, G. De Roeck, B. Peeters, *Parameterization of damage in reinforced concrete structures using model updating*, Journal of Sound and Vibration, Vol. 228, No. 4, Elsevier (1999), pp. 717-730.

[3] A. Teughels, J. Maeck, G. De Roeck, *Damage assessment by FE model updating using damage functions*, Computers & Structures, Vol. 80, No. 25, Elsevier (2002), pp. 1869-1879.

[4] A. Teughels, G. De Roeck, *Structural damage identification of the highway bridge Z24 by FE model updating*, Journal of Sound and Vibration, Vol. 278, No. 3, Elsevier (2004), pp. 589-610.

[5] V.-H. Nguyen, S. Schommer, S. Maas, A. Zürbes, *Static load testing with temperature compensation for structural health monitoring of bridges*, Engineering Structures, Vol. 127, Elsevier (2016), pp. 700-718.

[6] S. Schommer, *Damage detection in prestressed concrete bridges based on static load testing, sagging and modal parameters, using measurements and model updating*, PhD dissertation, University of Luxembourg, Luxembourg (2017).

[7] S. Schommer, V.-H. Nguyen, S. Maas, A. Zürbes, *Model updating for structural health monitoring using static and dynamic measurements*, In: Proc., X International Conference on Structural Dynamics, EURODYN 2017, Vol. 199, Elsevier (2017), pp. 2146-2153.